Evaluation and Characterization of Forage Sorghum as Feedstock for Fermentable Sugar Production

D.Y. Corredor[b], J.M. Salazar[c], K.L. Hohn[c], S.Bean[d] , B.Bean[e] and D. Wang[b,*]

[b] *Department of Biological and Agricultural Engineering, Kansas State University, Manhattan, KS 66506*
[c] *Department of Chemical Engineering, Kansas State University, Manhattan, KS 66506*
[d]*USDA-ARS Grain Marketing and Production Research Center, Manhattan, KS 66502*
[e] *Research and Extension Center, Texas A&M , Amarillo , TX, 79106*

Abstract

Sorghum is a tropical grass grown primarily in semiarid and drier parts of the world, especially areas too dry for corn. Sorghum production also leaves about 58 million tons of by-products composed mainly of cellulose, hemicellulose, and lignin. The low lignin content of some forage sorghums such as brown midrib makes them more digestible for ethanol production. Successful use of biomass for biofuel production depends on not only pretreatment methods and efficient processing conditions but also physical and chemical properties of the biomass. In this study, four varieties of forage sorghum (stems and leaves) were characterized and evaluated as feedstock for fermentable sugar production. Fourier transform infrared spectroscopy and X-ray diffraction were used to determine changes in structure and chemical composition of forage sorghum before and after pretreatment and the enzymatic hydrolysis process. Up to 72% of hexose yield and 94% of pentose yield were obtained using "modified" steam explosion with 2% sulfuric acid at 140°C for 30 min and enzymatic hydrolysis with cellulase (15 FPU/g. cellulose) and β-glucosidase (50 CBU/g. cellulose).

Keywords: Forage Sorghum, FTIR, XRD, Enzymatic Hydrolysis, Dilute Acid, Pretreatment.

---

[*] Corresponding author. Phone: 785-532-2919. Fax: 785-532-5825. Email: dwang@ksu.edu

Introduction

Ethanol derived from lignocellulosic materials has great potential to be a sustainable replacement for corn grain in production of transportation fuels and energy applications. Conversion of cellulosic biomass such as agricultural residues to fuels and chemicals offers major economic, environmental, and strategic benefits, and biological processing based on cellulases offers high sugar yields vital to economic success. The U.S. DOE and USDA projected that U.S. biomass resources could provide approximately 1.3 billion dry tons/year of feedstock for biofuels production, which could produce enough biofuels to meet more than one-third of annual U.S. fuel demand for transportation (1).

Sorghum is a tropical grass grown primarily in semiarid and drier parts of the world, especially areas too dry for corn. Sorghum produces 33% more dry mass than corn in dry land. About 14 million metric tons of sorghum grains (about 7.7 million acres) were produced in the United States in 2007, and more than 6 million acres of forage sorghum are planted each year, resulting in about 58 million tons of sorghum biomass (stems and leaves) composed mainly of cellulose, hemicellulose, and lignin (2). Forage sorghum, sometimes called “cane” has the potential to grow very tall (6 to 15 feet) and can produce a large amount of vegetative growth. Forage sorghums can produce as much, and in some cases more, dry matter than corn when grown with the same amount of water (3). Compared with corn, forage sorghum is cheaper to produce, has comparable yields, and has slightly lower forage quality for silage. These qualities give forage sorghum potential for use in ethanol production (4, 5). Although cellulosic biomass is receiving growing attention as a renewable feedstock, the concept is not well understood for sorghum biomass because scientific information on using forage sorghums such as brown midrib (BMR) for ethanol production is limited. In recent years, introduction of sorghum plants containing the BMR gene generated much interest because plants with this trait have lower lignin concentrations than conventional types (3). Researchers have used chemical and genetic approaches to improve forage fiber digestibility by reducing the amount of lignin or extent of lignin cross linked with cell wall carbohydrates. BMR forage genotypes usually contain less lignin and may have altered lignin chemical composition (4, 5). Varieties with low lignin content and less lignin cross linked with cell wall carbohydrates could be easily hydrolyzed to fermentable sugars.

Pretreatment, enzymatic hydrolysis, and fermentation are three major steps for ethanol production from lignocellulosic biomass. Successful use of biomass for biofuel production depends on four important factors: physical and chemical properties of the biomass, pretreatment methods, efficient microorganisms, and optimization of processing conditions. Pretreatment is cruicial; it releases cellulose from the lignocellulose matrix, hydrolyzes hemicellulose, breaks and/or removes lignin, and turns crystalline cellulose into an amorphous form (6, 7). Pretreatment methods have been extensively studied (6-11), as have efficient microorganisms and optimization of processing conditions (12-19). However, at present, there are few studies about physical and chemical characterization of biomass before and after pretreatment and hydrolysis (20-22).

Cellulose and hemicellulose are the main polymers found in biomass. They are polymers of hexoses (mannose, glucose, galactose) and pentoses (xylose and arabinose), respectively. The microstructure and properties of cellulosic biomass have significant effects on bioconversion rate. Crystallinity, morphology, and surface area accessible for cellulase binding are major physical and structural factors that affect pretreatment and enzymatic hydrolysis (23, 24). We found no reported information on pretreatment, enzymatic saccharification, and fermentation of forage sorghum for biofuel. Infrared spectroscopy and X-ray diffraction could be useful tools for rapidly obtaining information about the structure of forage sorghum constituents and chemical changes occurring in various treatments. Previously, these techniques have been used to study structure and morphology of plant carbohydrates and lignocellulose (22, 25-29). In this work, fourier transform infrared spectroscopy (FTIR) and X-ray Diffraction (XRD) were used to study changes in chemical composition and chemical structures after pretreatment and enzymatic hydrolysis. These processes were developed and optimized in previous studies to analyze the relationships among composition, microstructure, and fermentable sugars yield (30, 31). This work is part of a long-term project designed to study the feasibility of ethanol production from forage sorghum.

Materials and Methods

Materials

Four types of forage sorghum (stems and leaves) with 8% moisture content were evaluated. FS-3, BMR forage sorghum classified as a medium-early maturing hybrid, was obtained from Sharps Bros Seed, Manhattan, KS. FS-2 is a photoperiod sensitive, non-BMR sorghum/sudangrass. FS-1 is a photoperiod sensitive BMR forage sorghum (4 Evergreen BMR) from Walter Moss Seed Co. FS-R, obtained from Kansas State University, was used as a control; it was classified as normal forage sorghum. Sorghum biomass samples were stored at 4ºC. Chemical composition of these forage sorghums ranged from 24–38% cellulose, 12–22% hemicellulose, 17-20% lignin and 1–22% starch.

Total carbohydrate composition ranged from 59 - 66% (Table 1). All reported yields were normalized to the total potential glucose and xylose in the original untreated material to provide perspective on the relative contribution of each sugar to total sugar recovery. Cellulase (Celluclast 1.5 L, 90 FPU/ml) and Novozyme 188 (β-glucosidase) (250 CBU/ml) from Novozyme (U.S. Office: Franklinton, NC) were used for enzymatic hydrolysis of forage sorghum into fermentable sugars. Sugars used for High Performance Liquid Chromatography (HPLC) calibration were purchased from Fischer Scientific Inc. (Pittsburgh, PA).

Starch Degradation

To ensure complete removal of starch before pretreatments, Liquozyme and Spyrizime (U.S. Office: Franklinton, NC) were used for starch liquefaction and saccharification, respectively. A 20-L steam jacket kettle (Model TDC/2-10, Dover Corporation, IL) with 5 L of medium containing 10% forage sorghum dry matter (DM) and 20 μL/20 g starch of Liquozyme was heated (85°C) with agitation (140 rpm) (Barnant Mixer Model 750-0230, Barrington, IL) for 1 h at pH 5.8. After decreasing the temperature to 60°C, Spyrizime (100 μL/20 g starch) was added and saccharification was allowed to proceed for another 2 h at pH 4.5 with continuous agitation at 140 rpm. After saccharification, residual forage sorghum was centrifuged (Programmable Centrifuge Model IEC PR-7000M, International Equipment Company, Needham Heights, MA.) at 3760 *g* at room temperature for 10 min. Forage sorghum cake was freeze dried for 48 h and collected for further pretreatment and enzymatic hydrolysis.

Pretreatment with Dilute Acid and Modified Steam Explosion

The treatment was carried out in a 1-L pressure reactor apparatus (Parr Instrument Company, Moline, IL). Forage sorghum was mixed with dilute acid (2% H_2SO_4) to obtain 5% dry matter. The slurry (≈27 g forage sorghum/500 ml) was loaded into the reactor and treated at 140°C for 30 min, following the "modified" steam explosion procedure described by Corredor et al. (31). After treatment, the remaining solid was washed three times with 300 ml of hot deionized water (85ºC). To avoid irreversible collapse of pores within the biomass, pretreated samples were not dried before enzymatic hydrolysis (32). A portion of the washed sample was freeze dried for 48 h, and the solid was stored at 4°C for subsequent characterization. The washed, pretreated, wet solid was stored at 4°C for subsequent enzymatic hydrolysis. A liquid sample from the treatment and washing process was analyzed by HPLC for recovery sugars.

Enzymatic Hydrolysis

Pretreated forage sorghum was mixed with distilled water to obtain a solution with 10% solid content and then treated with a mixture of enzymes. Two commercial enzymes, Celluclast 1.5 L and Novozyme 188 (β-glucosidase), were used for hydrolysis of cellulose and hemicellulose in forage sorghum. Enzyme loading of cellulase and β-glucosidase was 15 FPU/g cellulose and 50 CBU/g cellulose, respectively. Enzymatic hydrolysis was carried out in flasks with 100 ml of slurry at 45°C and pH 4.8 for 12 to 96 h in a water-bath shaker with an agitation speed of 140 rpm. Sodium azide (0.3% w/v) was used to inhibit microbial growth during the enzymatic hydrolysis. Samples were taken out each 12 h for sugar analysis. After enzymatic hydrolysis, samples were heated at 100°C for 15 min and stored at 4°C to inactivate the enzymes. Unhydrolized forage sorghum was separated by centrifuging at 13500 *g* for 10 min at room temperature. Liquid was collected for sugar analysis.

Analytical Methods

Cellulose and hemicellulose of forage sorghum were analyzed by Filter Bag Technology (ANKOM Technology, Macedon, NY). Total lignin was determined using laboratory procedures developed by the National Renewable Energy Laboratory (32). Starch content was determined using commercially available kits from Megazyme (Bray, Ireland) according to AACC Approved Method 76-13 (33). Protein was determined via nitrogen combustion using a LECO FP-528 nitrogen determinator (St. Joseph, MI) according to AACC Approved Method 46-30. Nitrogen values were converted to protein content by multiplying by 6.25. Crude fiber, fat, and ash were determined by AOAC standard methods (34).

Concentrations of sugars were determined by HPLC using an RCM-monosaccharide column (300 x 7.8 mm; Bio-Rad, Richmond, CA) and refractive index detector. Samples were neutralized with $CaCO_3$, run at 85°C, and eluted at 0.6 ml/min with distilled water. Hexose yield was counted as the final amount of glucose derived from cellulose. Pentose yield was counted as the final amount of pentose sugars derived from hemicellulose.

Forage sorghum before and after treatments were analyzed by XRD in a Bruker AXS D-8 difractometer settled at 40 KW, 40 mA; radiation was cupper Kα (λ= 1.54 Å); and grade range was between 5 to 40° with a step size of 0.03°. Aperture, scatter, and detector slits were 0.3°, 0.3°, and 0.03°, respectively. Presence of crystallinity in a sample can be detected by absorption peaks. Crystallinity index (CrI) was calculated using the method of Segal et al. (35). CrI is determined by the ratio of the maximum intensity of the peak at the 002 lattice diffraction (in arbitrary units) or “crystalline” peak to the intensity of the “amorphous” peak in the same units at $2\theta = 18°$. Images of the surfaces of pretreated and untreated forage sorghum were taken at magnifications from 1.5K to 3K using a Hitachi S-3500 N scanning electron microscope (SEM). Specimens were mounted on conductive adhesive tape; sputter coated with gold palladium, and observed using a voltage of 15 to 20 kV.

FTIR measurement was performed in the original and treated forage sorghum using a Thermo Nicolet Nexus™ 670 FT-IR spectrophotometer equipped with a Smart Collector. Reagent KBr and samples were dried for 24 h at 50°C and then prepared by mixing 2 mg of sample with 200 mg of spectroscopy grade KBr. The analysis was carried out in the wavenumber range of 400–4000 cm^{-1}, with detector at 4 cm^{-1} resolution and 32 scans per sample. OMNIC 6.1a software (Thermo-Nicolet Corporation, Madison, WC) was used to determine peak positions and intensities.

Analysis of variance (ANOVA) and least-significant difference (LSD) were done using SAS (SAS Institute 2005, Cary, NC).

Results and Discussion

Fourier Transform Infrared Spectra

Table 2 summarizes FTIR results for the forage sorghum samples during treatments. Figure 1 shows FTIR spectra of untreated samples in the wavelength region from 3800 - 900 cm^{-1}; Figures 2, 3 and 4 show FTIR spectra of untreated samples after treatment and after enzymatic hydrolysis in the fingerprint region of 1800 to 900 cm^{-1}. IR spectra of untreated forage sorghum show a strong bands associated with hydrogen bonded O-H stretching absorption around 3300 cm^{-1} and a prominent C-H stretching absorption around 2900 cm^{-1}. (Fig. 1) (36). In the fingerprint region, between 1800-900 cm^{-1}, many absorption bands associated with various contributions from vibrations modes in carbohydrates and lignin are also present in forage sorghum (36, 37). Differences between hardwood and softwood lignin also can be observed in the fingerprint region (37). Each sample shows a distinctly different pattern of absorbance. Close inspection of the peaks shows a peculiar hemicellulose band at 1732 cm^{-1} for all original samples. In cell walls, this peak has been related to saturated alkyl esters from hemicellulose (23, 36, 38, 39). The FTIR spectrum is not discernible after treatment, which indicates that hemicellulose is almost extracted by the pretreatment applied. Solubilization of pectins and some phenolics from the wall is also accompanied by changes in the 1245 cm^{-1} region and associated with changes in the 1732 cm^{-1} region (38). Changes around the 1245 cm^{-1} region have been related to C-O-H deformation and C-O stretching of phenolics plus an asymmetric C-C-O stretching of esters depending on the attached group (38). This band (1242-1247 cm^{-1}) is obvious in untreated samples and changes following the same behavior as the 1732 cm^{-1} peak. Bands at these wavelengths showed a broad peak in untreated samples that fades after treatment, confirming solubilization of phenolics and remotion of esters from the cell wall.

Important phenolic peaks are observed as a doublet at 1604 to 1638 cm^{-1} in all samples after treatment. The band at 1638 cm^{-1} is assigned to an aromatic stretch, and the band at 1604 cm^{-1} appears associated with the α-β double bond of the propanoid side group in lignin-like structures (38). Bands at 1604 and 1638 cm^{-1} are defined after pretreatment, weaken in samples FS-2 and FS-1 after enzymatic hydrolysis, and remain in samples FS-3 and FS-R. This suggests that treatments in samples FS-3 and FS-R did not completely remove lignin but were more effective in samples FS-2 and FS-1. This also is supported by presence of peaks at 1710-1712 cm^{-1} after treatment in all forage sorghum samples, which indicate C=O linkages of phenyl esters from remained lignin (36, 39).

Forage sorghum, a grass species, has two types of lignin (guaiacyl and syringyl rings), and softwood lignin almost exclusively contains guaiacyl rings (37, 40). These rings are seen as aromatic skeletal vibrations of the benzene ring at 1510 cm^{-1} bands (23, 36, 37, 41) and sometimes shifted toward a higher wave number (>1510 cm^{-1}) in softwoods (37). Guaiacyl ring-related IR spectra are present in all untreated samples at 1516-1517 cm^{-1} and have a strong peak in FS-3 and FS-2. The spectra remain after treatment and are still seen after enzymatic hydrolysis with a weak band in FS-3 and FS-R. Bands around 1460 cm^{-1} are attributed to C-H methyl and methylene deformation common in hardwoods, and bands at 1315 cm^{-1} are attributed to C-O absorption of syringyl rings in lignin (36, 37). The presence of syringyl units in forage sorghum is evident from the bands at 1453-1456 cm^{-1}, which have a weak absorption in untreated and treated samples but remain weak in FS-R and FS-3 after enzymatic hydrolysis. The same behavior is seen in the 1315-1317 cm^{-1} spectrum, which is well defined in FS-2 and FS-R after pretreatment; however, after enzymatic hydrolysis, these bands almost disappear. This suggests that FS-2 is composed mainly of guaiacyl rings, but FS-R, FS-3, and FS-1 have both syringyl and guaiacyl rings. After treatment, remotion of guaiacyl rings was more effective in FS-2 than other samples, maybe because of the strong presence of interaction among syringyl and guaiacyl rings on them.

Proteins give rise to two bands in the IR arising from the amide linkage. These bands are seen at about 1653 cm^{-1} (amide I) and 1549 cm^{-1} (amide II), often with an intensity ratio of about 2:1 (38). These bands are well defined in untreated FS-3, the sample with higher protein content (7.46%) (Table 1). The corresponding bands in other samples are weak but serve as confirmatory evidence of protein content in untreated samples. These bands disappear after treatment, suggesting that protein is removed with treatment.

Cellulose-related bands in the FTIR spectra are seen around 1430, 1370, 1162, 1098 and 900 cm^{-1} (23, 37, 41, 42). Bands around 1430 cm^{-1} are higher in softwood and related to C-H in plane deformation (asymmetric) of cellulose (37). These bands (1426-1429 cm^{-1}) are well defined in untreated FS-3 but weak in other samples. After treatment, bands are well defined in all samples and strong in FS-3. This suggests that FS-3 is composed mainly of deformation (asymmetric) of cellulose common in softwoods. The absorbance at 900 cm^{-1} is associated with the anti-symmetric out-of-phase ring stretch of amorphous cellulose (41, 43), and the 1098 cm^{-1} band is related to C-O vibration of crystalline cellulose (41). Both the crystalline (1098-1109 cm^{-1}) and amorphous (897-900 cm^{-1}) bands increase in intensity after pretreatment for all samples. However, bands of crystalline cellulose are more intense for FS-2 and FS-R, suggesting that these two samples have a higher percentage of crystalline cellulose after treatment, which is difficult to further hydrolyze with enzymes. These results indicate that treatment was more efficient at transforming crystalline cellulose to amorphous cellulose in FS-3 and FS-1 than in FS-2 and FS-R. The appearance of crystalline and amorphous peaks also indicates that cellulose is exposed because of the pretreatment applied. After enzymatic hydrolysis, there is still a weak peak of crystalline cellulose in FS-3 and FS-R; bands of amorphous cellulose appear weak in all samples, suggesting that amorphous cellulose is almost degraded with enzymes but crystalline cellulose remains in FS-3 and FS-R. Enzymatic hydrolysis likely degraded almost all amorphous cellulose in FS-2 and FS-1.

C-H deformation (symmetric) of cellulose is indicated in bands at 1372 cm^{-1} (37, 41). This peak appears around 1370-1375 cm^{-1} in all untreated samples with a weak signal in FS-1. After treatment, the band decreases in intensity and switches to 1366 cm^{-1} in all samples; however, it almost disappears after enzymatic hydrolysis and shows a weak band in FS-3. The decrease of this band after treatment suggests that cellulose is degraded because of the pretreatment applied and also hydrolyzed after enzymatic hydrolysis. The mainly antisymmetric stretching C-O-C glycoside in cellulose is seen around the 1162 cm^{-1} region (23, 37, 41). This antisymmetric C-O-C vibration is well defined in all treated samples (1159-1162 cm^{-1}) and turns in a flat peak after enzymatic hydrolysis. The decrease in this peak intensity could be related to degradation of β,1-4 glycosil linkages of cellulose due to enzymatic hydrolysis. Finally, peaks around 1058 cm^{-1} and 1035 cm^{-1} seem to be well defined after treatment in all samples, but they completely disappear after enzymatic hydrolysis. Those peaks are related to C-O stretching of cellulose (37). This confirms that cellulose is fully exposed to further enzymatic hydrolysis after treatment and this procedure is efficient in degrading cellulose to its monomeric sugars.

Morphological Structure

Morphological features of untreated forage sorghum samples after treatment and enzymatic hydrolysis are shown in Figures 5, 6 and 7. Untreated samples seem to have of deposits on the surface (Fig. 5a). This surface layer can include waxes, hemicellulose, lignin, and other binding materials and has also been observed in corn stover, sorghum leaves and stems, and wheat straw (23, 44, 45). We can also observe some internal plant structures such as vascular bundles and holes in the cellulose wall used for ventilation and metabolism (Fig. 5.b and c) (46). The general particle size of untreated samples is from 50 to 100μm., The surface layer is removed during treatment, resulting in total exposure of internal structure and fibers that have a relatively clean and smooth surface as shown in Figure 6b and c. We can observe some annular rings (Fig. 6c) and macro fibrils, probably composed of single cells held together to form a fiber bundle (Fig. 6b). These images confirm that outer layers are degraded and internal structures, including cellulose, are fully exposed after treatment. An SEM image of the sample after enzymatic hydrolysis shows that the compacted outer layer was removed (Fig. 7b). The image also shows some well-defined micro fibers (5-16 μm of diameter), which might be evidence that cellulose fibers are agglomerates of individuals cellulose microfibers (Fig. 7a and c). This result is in agreement with previous reports in which cellulose particles existed as aggregates of crystalline cellulose entities (44, 46). However, these fibers appeared in some samples with serrations at the edge and are still connected together with neighboring fibers by some amorphous material, probably unremoved hemicellulose (Figure 7b). No previous reports are available on the dimensions of single fibers in forage sorghum; however, we can observe that after enzymatic hydrolysis, particle size reduced notably to elements of about

60 µm length and 5 to 6 µm width. This also suggests that enzymatic hydrolysis reduced and degraded cellulose, leaving a small final solid that might need further degradation.

X-Ray Diffraction

Figure 8 shows the XRD spectra of untreated samples, the pretreated sample, and the remaining solids after enzymatic hydrolysis. Spectra show the ordered arrangement of the glucan chains that regulate the physical and chemical characteristics of cellulose. These bonds not only present a regular crystalline arrangement of the glucans molecules resulting in distinct X-ray diffraction patterns but also relate to the swelling and reactivity of cellulose (47). The ratio of intensity of crystalline and amorphous diffractions is approximately equal to the ratio of the masses of amorphous and crystalline parts of a polymer (48). In untreated FS-3 and FS-1, we observe an amorphous XRD pattern that predominates over the crystalline one, probably because of the presence of a high content of amorphous cellulose and/or amorphous materials (including hemicellulose). For untreated FS-2 and FS-R, the crystalline peak predominates and is well defined at common scale. This could support the hypothesis of differences between cellulose crystallinity among samples. It seems that untreated FS-2 and FS-R have high crystalline cellulose content, which could be difficult for transformation to amorphous cellulose with treatments and for further hydrolysis to sugars.

After pretreatment, the main peak relative to plane 002 is easily observed in all treated samples, showing that the amount of cellulose increased because of the removal of lignin and hemicellulose. This also confirms that pretreatment is effective in exposing cellulose to enzymatic attack. Furthermore, the crystalline peak is higher in intensity for

FS-R and FS-2, suggesting that these samples have higher content of crystalline cellulose than amorphous cellulose after pretreatment. This provides additional confirmation of the FTIR analysis results, which showed that bands of crystalline cellulose were more intense for FS-2 and FS-R after treatment. Low intensity of crystalline peaks in FS-3 and FS-1 suggests that pretreatment was effective at transforming crystalline to amorphous cellulose in these samples and that enzymatic hydrolysis will be easy for these samples because they have higher amounts of amorphous cellulose. XRD of samples after enzymatic hydrolysis shows that the cellulose content decreased. The greatest change was observed in FS-3, but some well-defined crystalline peak remains in FS-2 and FS-R. The crystallinity pattern of FS-1 after enzymatic hydrolysis looks similar to its pattern before treatment, suggesting that enzymatic hydrolysis is more effective at hydrolyzing amorphous cellulose in FS-3 and FS-1 than in FS-2 and FS-R, probably because of the original type of cellulose.

We can verify these assumptions of effective hydrolysis of amorphous cellulose in samples by calculating the crystallinity index of untreated forage sorghum (CrI) using the method of Segal et al. (35) after treatment and after enzymatic hydrolysis (Table 3). Lower crystallinity has been associated with cellulose decrystallization as well as high value to amorphous material (23, 44). CrI values for FS-2 and FS-R are always higher (47-49%), even after enzymatic hydrolysis (50 – 75%), than for FS-4 and FS-1. This means that the crystalline fraction in FS-2 and FS-R is higher than the amorphous fraction. After pretreatment, all samples show almost the same degree of crystallinity (51-58%). However, after enzymatic hydrolysis, the crystalline peak is almost degraded for FS-3 and FS-1, as noticed from the decreased degree of crystallinity to 16 and 35%, respectively. This confirms that applied procedures easily decrystallize and degrade cellulose in FS-3 and FS-

1. Profiles of the diffractograms are in agreement with previously reported results for mycro-crystalline cellulose samples (49, 50).

Pentoses and Hexoses Yield

Steam explosion with 2% H_2SO_4 at 140°C for 30 min gives a maximum pentose yield of 93% from FS-2 and a minimum pentose yield of 80% from FS-R forage sorghum. Pretreatment is more efficient at hydrolyzing hemicellulose in FS-2 and FS-3 than in FS-R and FS-1 (Fig. 9). No hexose yield is reported because no significant amounts of hexoses were found after treatment. Although FS-2 has a medium content of hemicellulose (17.7%) (Table 1), this sample gives the maximum yield of pentose sugars followed by FS-3. However, FS-R and FS-1, which have high amounts of hemicellulose (20.4 and 22.4%, respectively) give low pentose yields (84 and 79%, respectively). Based on FTIR analysis, we can suggest that not only hemicellulose and lignin contents affect hydrolysis of hemicellulose but the almost exclusive presence of guaiacyl rings of lignin also affects hemicellulose degradation. The presence of these rings could facilitate effortless degradation of lignin and further hydrolysis of hemicellulose as seen in FS-2 and FS-3.

A maximum hexose yield of 79% is obtained from FS-3 after 72 h of enzymatic hydrolysis (Fig. 10). FS-2 and FS-R have the lowest hexose yields (43 and 48%, respectively) after 72 h of enzymatic hydrolysis. The higher hexose yield obtained from FS-3 and FS-1 corresponds with results obtained from XRD and FTIR analysis. The ordered arrangement of the glucan chains with a dominated amorphous pattern in FS-3 and FS-1 facilitated hydrolysis of cellulose to monomeric sugars in these samples. These results also support the idea of decrystallization and hydrolysis of cellulose after enzymatic hydrolysis for FS-3 and FS-1, probably because the initial ordered arrangement controls the swelling and reactivity of cellulose.

Conclusion

Four varieties of forage sorghum with carbohydrate content ranging from 59 to 66% and cellulose content ranging from 24 to 38% were evaluated as potential feedstocks for bio-ethanol production. FTIR, SEM, and XRD were used to characterize the physical and chemical properties of forage sorghum as affected by pretreatment and enzymatic hydrolysis. There is strong relationship among chemical structure, function, composition, and fermentable sugars yield. Up to 72% of hexose yield from FS-3 and 94% of pentose yield from FS-2 were obtained using modified steam explosion with 2% sulfuric acid at 140°C for 30 min and enzymatic hydrolysis with cellulase (15 FPU/g. cellulose) and β-glucosidase (50 CBU/g. cellulose). Forage sorghums with a high percentage of guaiacyl rings in their lignin structure were easy to hydrolyze after pretreatment despite the initial lignin content. Pretreatment was more effective for forage sorghums with a low crystallinity index and easily transformed crystalline cellulose to amorphous cellulose, despite initial cellulose content. Additional studies on ethanol fermentation of low lignin content or modified pretreated forage sorghum are needed.

Acknowledgements

We would particularly like to acknowledge the support from Kansas State Agricultural Experiment Station, Kansas State University, Manhattan, KS. Contribution no. 08-337-J from the Kansas Agricultural Experiment Station.

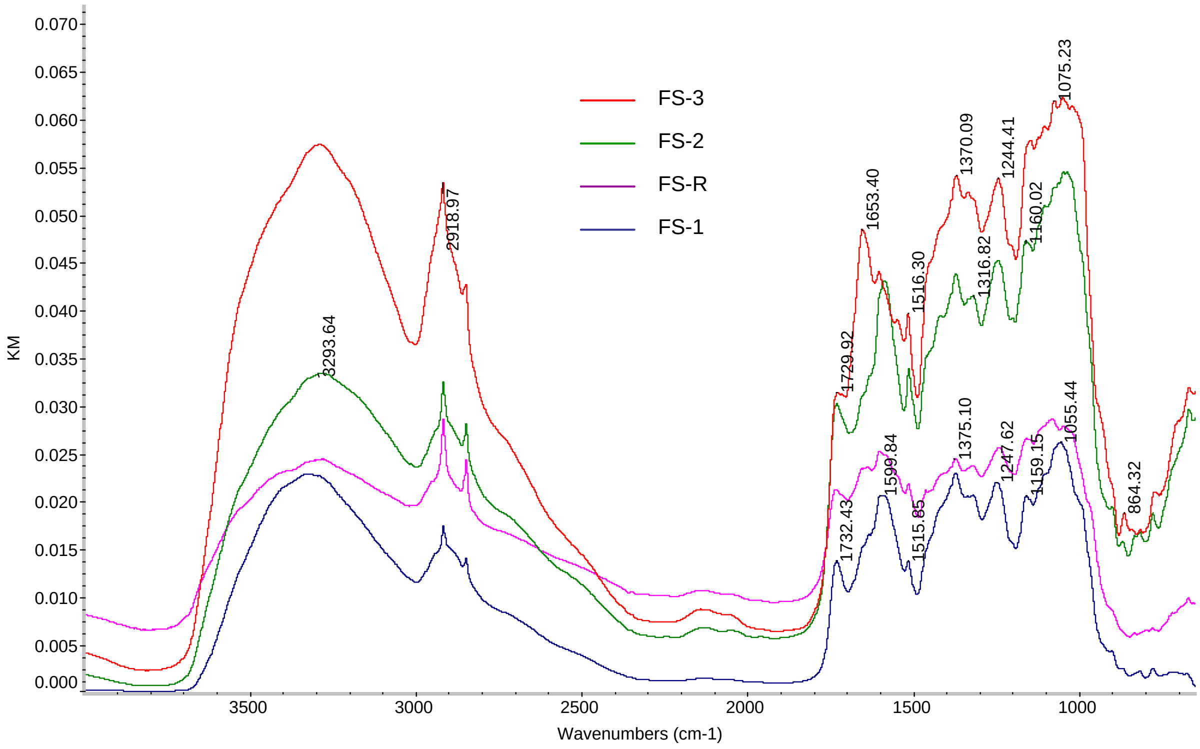

Fig. 1 FTIR spectra of untreated forage sorghums

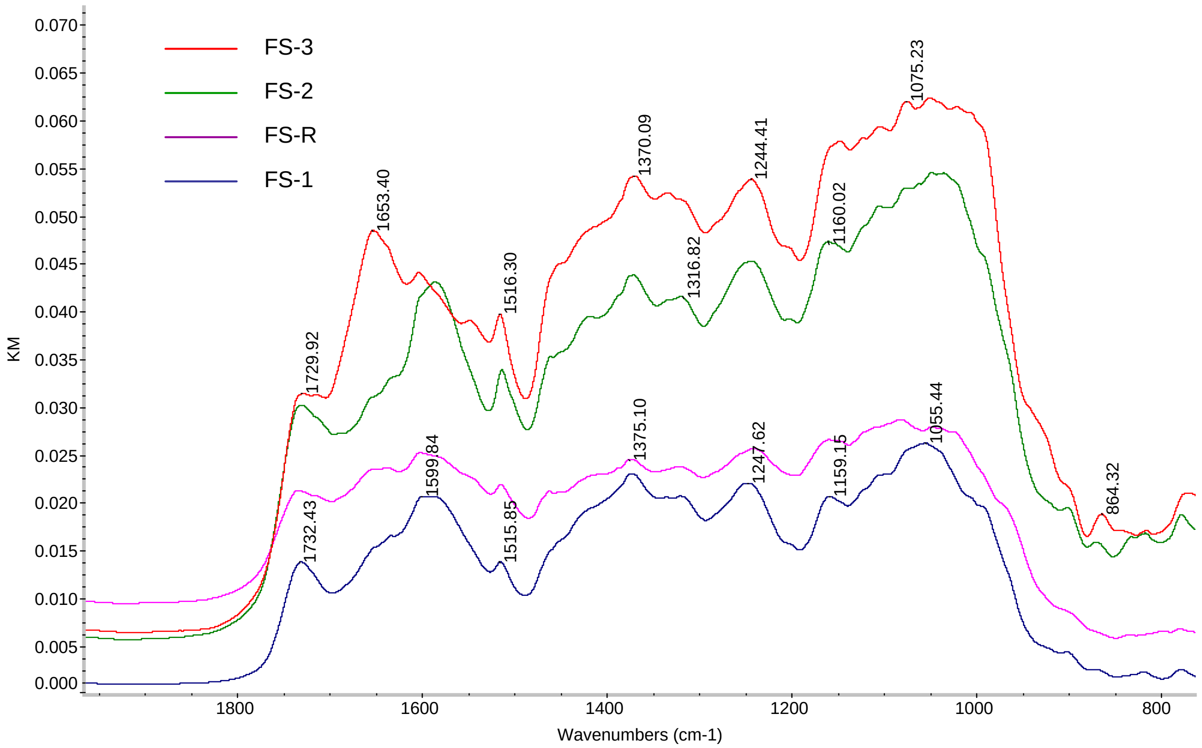

Fig. 2 FTIR spectra of untreated forage sorghums in the fingerprint region (900 – 1800 cm^{-1}).

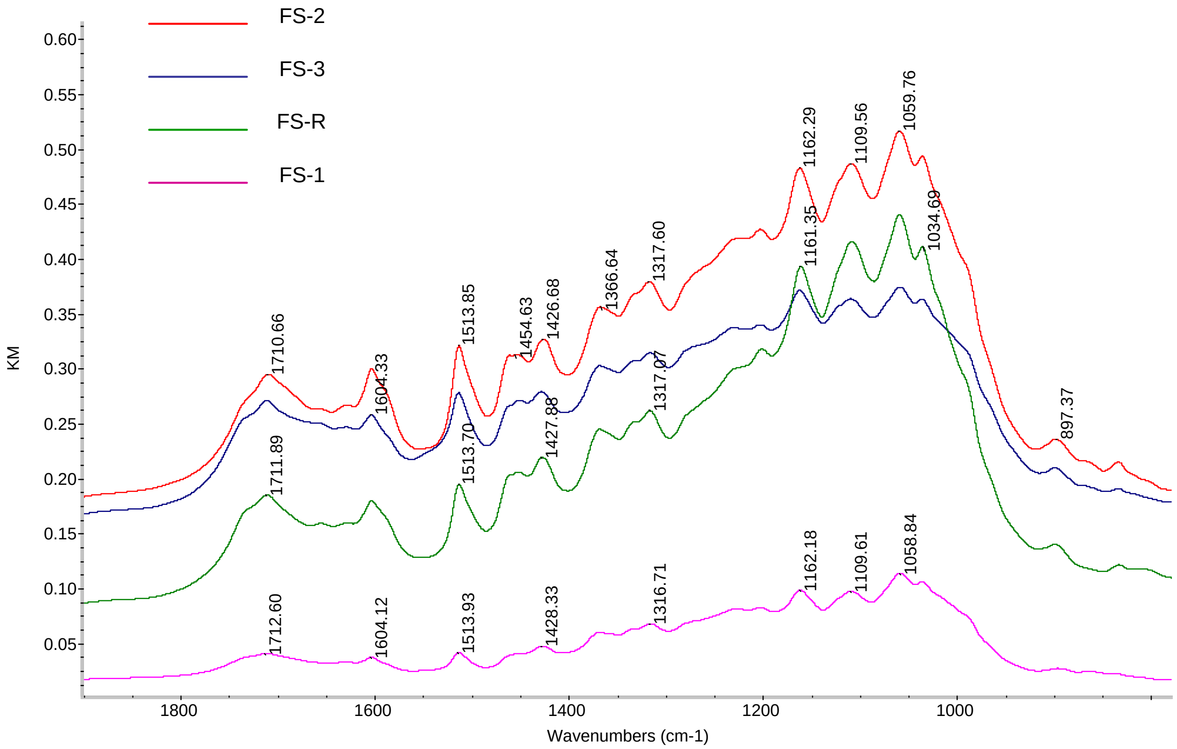

Fig. 3 FTIR spectra of forage sorghums after dilute acid and modified steam explosion pretreatment in the fingerprint region (900 – 1800 cm^{-1}).

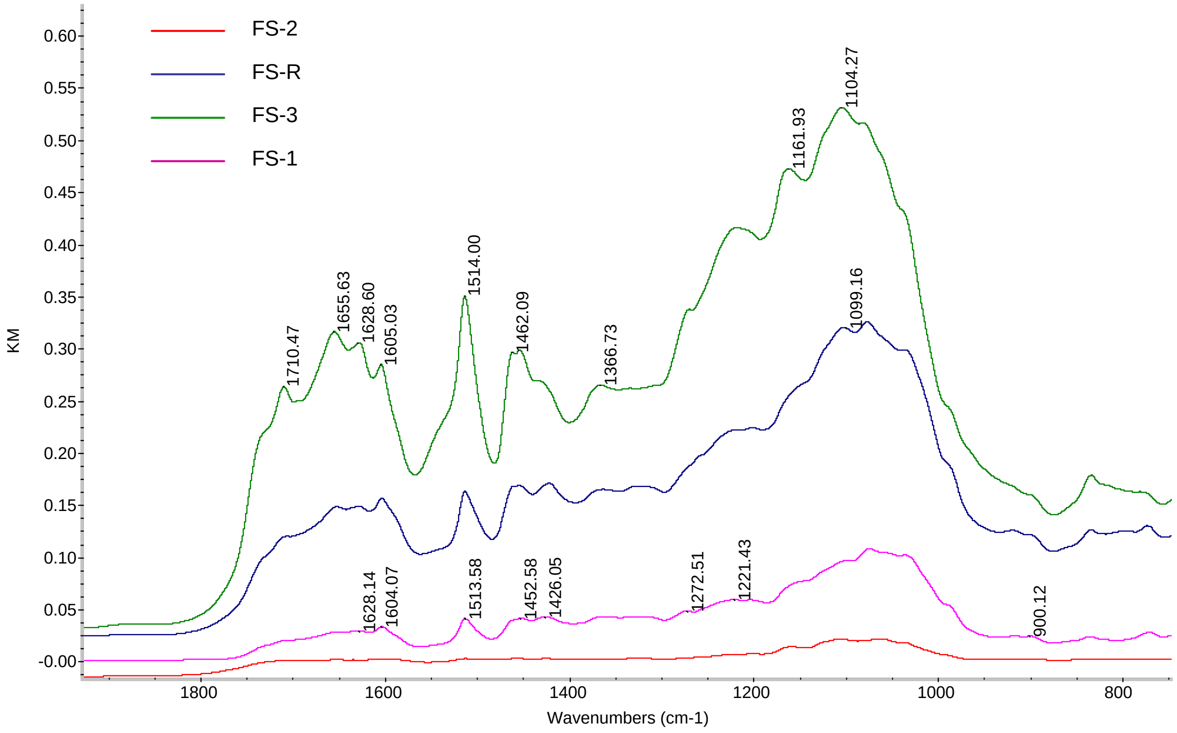

Fig. 4 FTIR spectra of forage sorghums after enzymatic hydrolysis in the fingerprint region (900 – 1800 cm^{-1}).

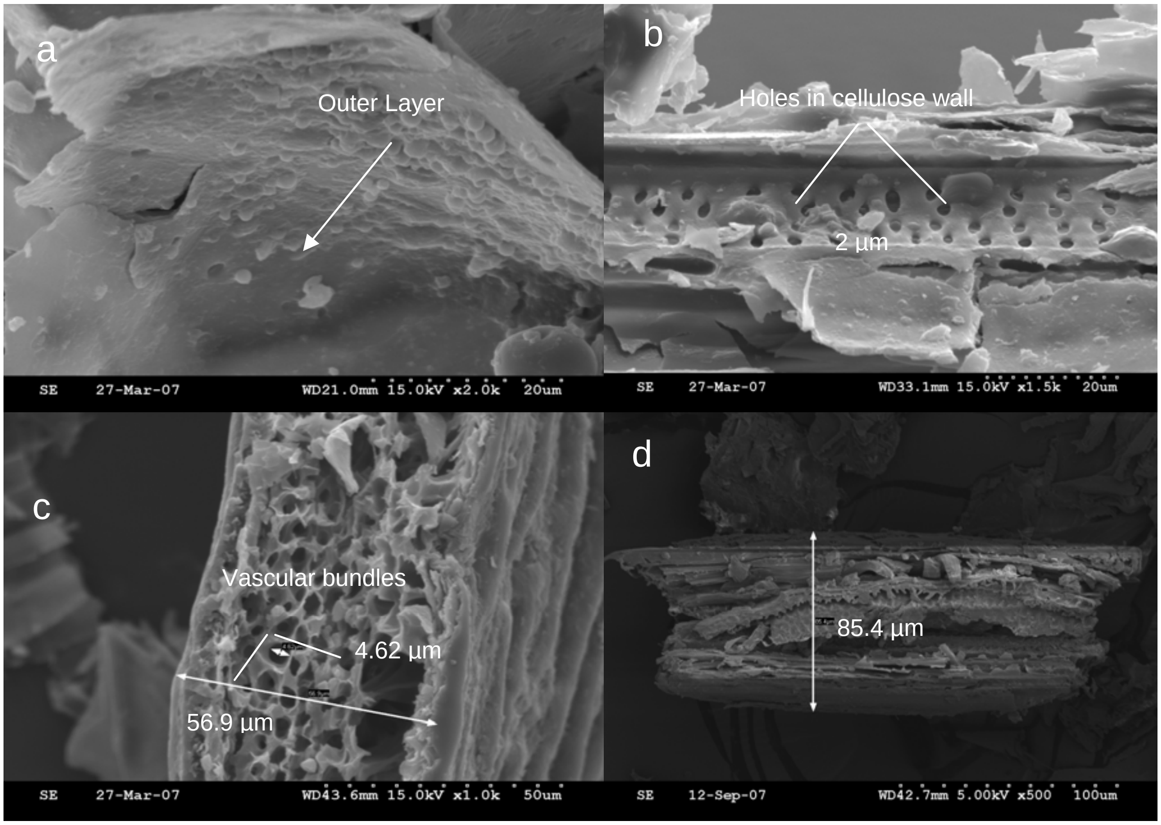
a
Outer Layer
SE 27-Mar-07 WD21.0mm 15.0kV x2.0k 20um
b
Holes in cellulose wall
2 µm
SE 27-Mar-07 WD33.1mm 15.0kV x1.5k 20um
c
Vascular bundles
4.62 µm
56.9 µm
SE 27-Mar-07 WD43.6mm 15.0kV x1.0k 50um
d
85.4 µm
SE 12-Sep-07 WD42.7mm 5.00kV x500 100um

Fig. 5 SEM images of untreated sorghum forages a) FS-3; b) FS-2; c) FS-1; d) FS-R.

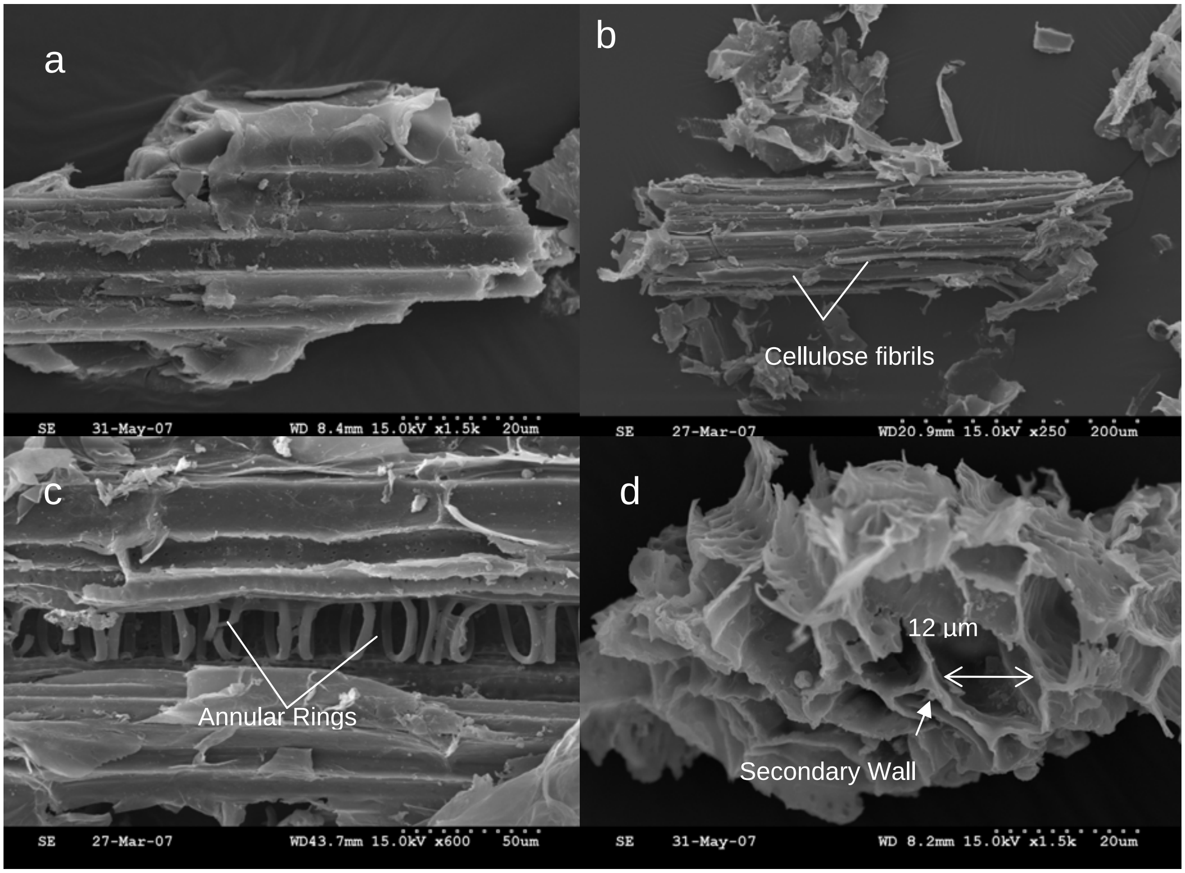
a
SE 31-May-07 WD 8.4mm 15.0kV x1.5k 20um
b
Cellulose fibrils
SE 27-Mar-07 WD20.9mm 15.0kV x250 200um
c
Annular Rings
SE 27-Mar-07 WD43.7mm 15.0kV x600 50um
d
12 µm
Secondary Wall
SE 31-May-07 WD 8.2mm 15.0kV x1.5k 20um

Fig. 6 SEM images of treated forage sorghums with dilute acid and modified steam explosion pretreatment a) FS-3; b) FS-2; c) FS-1; d) FS-R

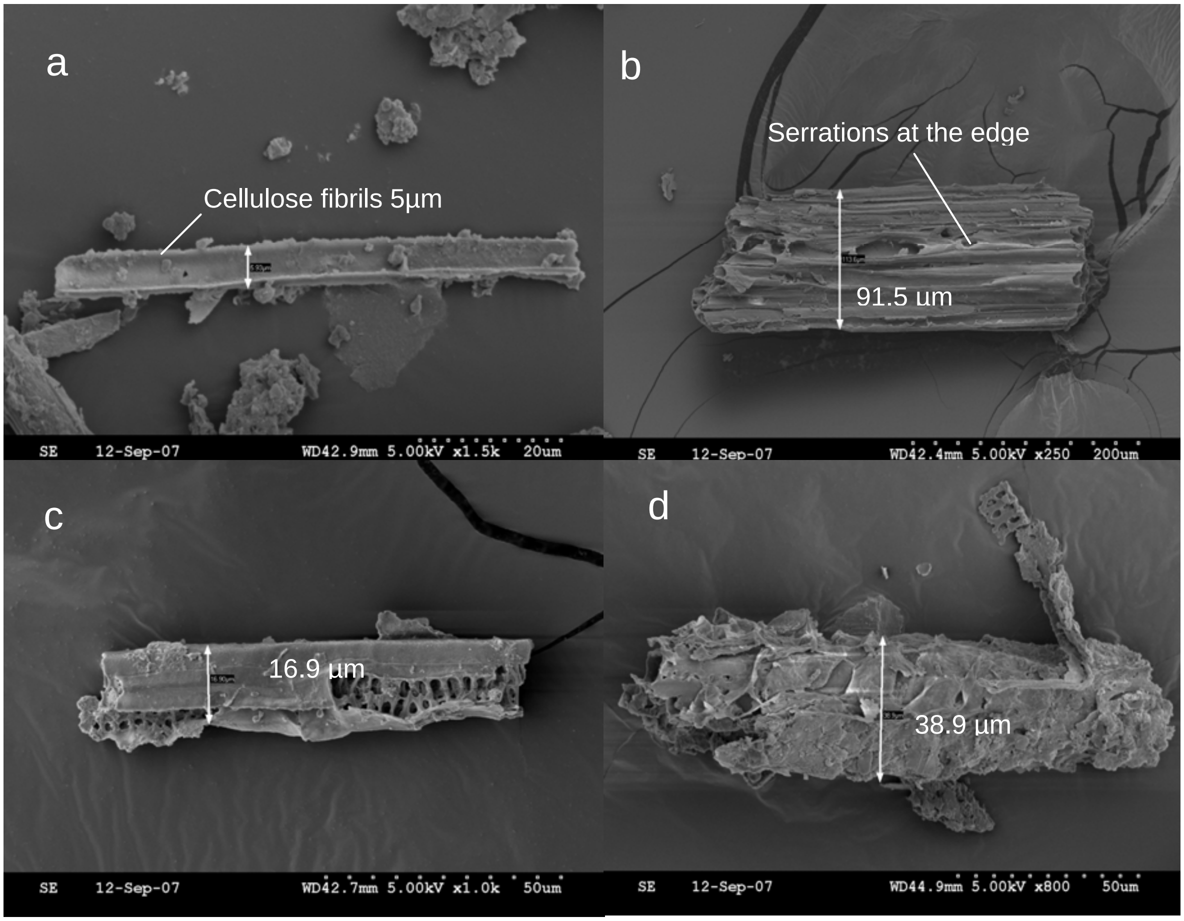
a
Cellulose fibrils 5µm
SE 12-Sep-07 WD42.9mm 5.00kV x1.5k 20um
b
Serrations at the edge
91.5 um
SE 12-Sep-07 WD42.4mm 5.00kV x250 200um
c
16.9 µm
SE 12-Sep-07 WD42.7mm 5.00kV x1.0k 50um
d
38.9 µm
SE 12-Sep-07 WD44.9mm 5.00kV x800 50um

Fig. 7 SEM images of forage sorghums after pretreatment and enzymatic hydrolysis a) FS-3; b) FS-2; c) FS-1; d) FS-R

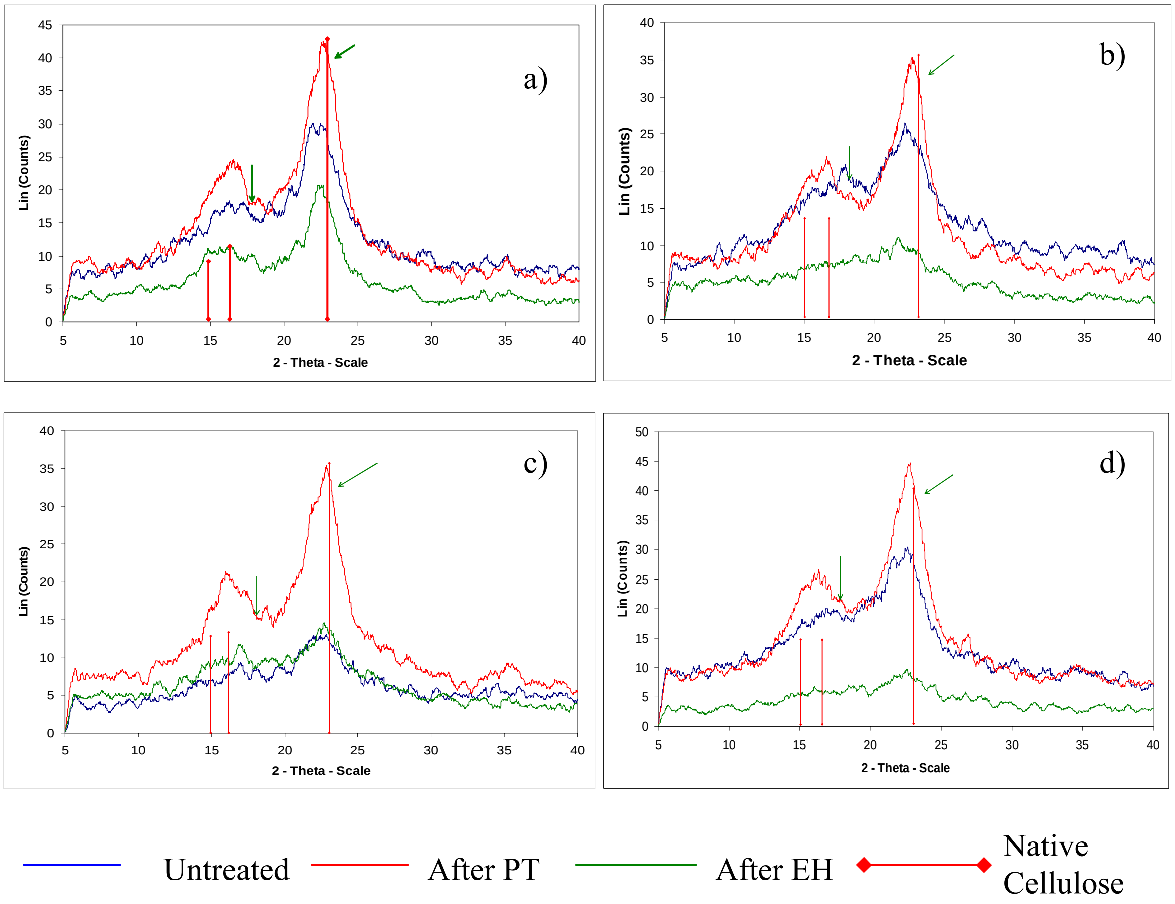

Fig. 8 X-ray diffraction of untreated forage sorghums after pretreatment and enzymatic hydrolysis a) FS-2; b) FS-3; c) FS-1; d) FS-R. The labeled peaks are the principal 002 peak (100% intensity) and 101 peak of native cellulose.

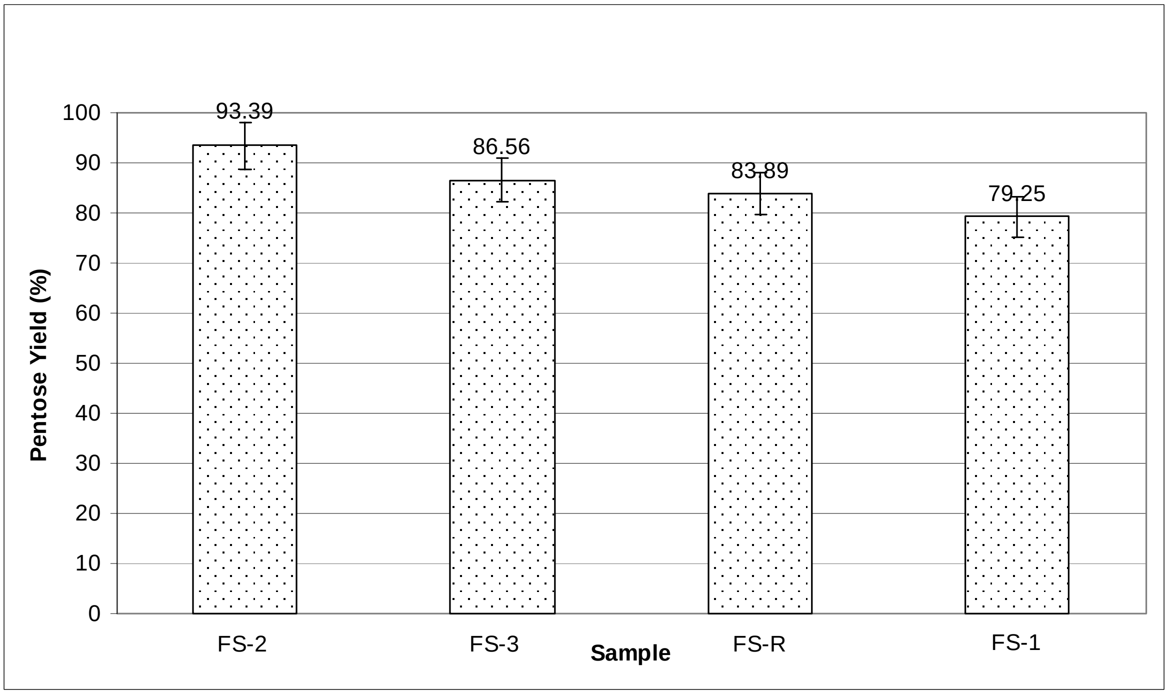

Fig. 9 Pentose yield (%) of forage sorghum after pretreatment with 2% H_2SO_4 at 140°C for 30 min.

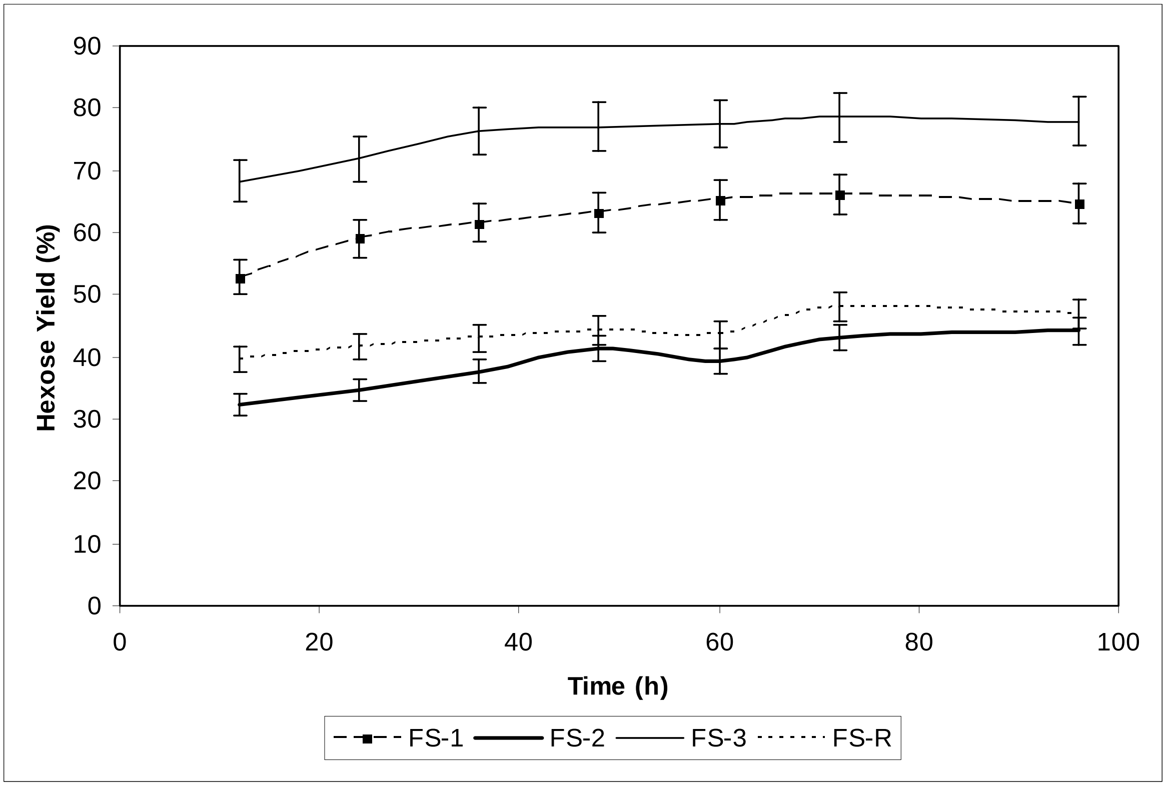

Fig. 10 Effect of enzymatic hydrolysis time on hexose yield for pretreated forage sorghums. Enzymatic hydrolysis was carried out with cellulase loading of 15 FPU/g cellulose and β-glucosidase 50 CBU/g cellulose at 45°C and pH 4.8

Table 1. Chemical composition of forage sorghums.

Component [a]	Sample			
	FS –1	FS -2	FS -3	FS - R
Carbohydrates	66.22	62.48	59.44	59.93
Starch	8.13b	6.80c	22.91a	0.84d
Hemicellulose	22.48a	17.64c	12.32d	20.37b
Cellulose	35.51b	38.04a	24.21c	38.72a
Total amount of Lignin[b]	13.46b	16.51a	13.58b	16.79a
Klason Lignin	14.63bc	19.14ab	11.06c	20.47a
Crude Fat	1.08b	1.07b	1.68a	1.14b
Crude Fiber	34.02b	36.87a	20.80d	29.43c
Crude Protein	5.16b	4.13c	7.46a	3.88d
Ash	9.29c	10.87a	6.93d	9.98b

[a] Means of two replications. Values in the same row with the same letters are not statistically different at $p<0.05$

[b] Calculated as AIL+ASL

Table 2. Assignment of the main bands in FTIR spectra for forage sorghums

Wavenumber (cm-1)	Common Pattern	Assignment	Reference
1732	Untreated Samples	Alkyl esther from cell wall hemicellulose C=O; Strong carbonyl groups in branched hemicellulose	(23, 37-39)
1710-1712	Well defined after PT	C=O in phenil ester from lignin	(39)
1653 and 1549	Untreated Samples	Protein strong band of amide I and amide II, respectively.	(38)
1638-1604	Well defined after PT	Doublet phenolics of remained lignin	(38)
1517-1516	Untreated Samples	Aromatic C-O stretching mode for lignin; Guayacyl ring of lignin (softwood).	(23, 26, 37)
1453-1456	Well defined after PT	Syringil absorption of hardwoods (C-H methyl and methylene deformation).	(37)
1426-1429	Well defined after PT	C-H vibrations of cellulose ; C-H deformation (asymmetric) of cellulose	(26, 37, 41)
1370-1375	Untreated Samples	C-H Stretch of cellulose	(23, 41)
1315-1317	Untreated Samples	C-O Vibration of Syringil ring of lignin.	(37, 51)
1242-1247	Untreated Samples	C-O-H deformation and C-O stretching of phenolics.	(38, 41)
1159-1162	Well defined after PT	Antysimetric stretching C-O-C glycoside; C-O-C b-1,4 glycosil linkage of cellulose.	(23, 42, 43)
1098- 1109	Well defined after PT	C-O vibration of crystalline cellulose; Glucose ring strech from cellulose	(37, 41)
1060 and 1035	Well defined after PT	C-O vibrations of cellulose.	(41)
897-900	Well defined after PT	Amorphous cellulose vibration; Glucose ring strecth	(37, 41)

Table 3. Crystallinity Index (CrI) for forage sorghums[a].

Sample	Untreated	After PT	After EH
FS-1	38	52	35
FS-2	49	57	75
FS-3	36	51	16
FS-R	47	58	50

[a] Means of two replicates

References

[1] Perlack, R.D., Wright L.L., Turhollow A.F., Graham R.L., Stokes B.J., and Erback D.C. (2005) Biomass as feedstock for bioenergy and bioproducts industry: Technical feasibility of a billion-ton annual supply. Available from: http://feedstockreview.ornl.gov/pdf/billion_ton_vision.pdf. Accessed January 2008.

[2] United States Department of Agriculture. (2008) Data and Statistics. Available from: http://www.usda.gov/wps/portal/!ut/p/_s.7_0_A/7_0_1OB?navid=DATA_STATISTICS&parentnav=AGRICULTURE&navtype=RT. Accessed February 2008.

[3] Marsalis, M.A. (2004), PhD Thesis, Texas Tech University, Lubbock, USA.

[4] Oliver, A.L., Pedersen, J.F., Grant, R.J. and Klopfenstein, T.J. (2005) *Crop Sci.* 45, 2234-2239.

[5] Oliver,A.L., Pedersen,J.F., Grant,R.J., Klopfenstein,T.J. and Jose,H.D., (2005) *Crop Sci.* **45** 2240-2245.

[6] Saha,B.C., (2003) *J. Ind. Microbiol. Biotechnol.* **30** 279-291.

[7] Saha,B.C., (2004) *ACS Symp. Ser.* **889** 2-34.

[8] Abbas,C., Beery,K., Dennison,E. and Corrington,P., (2004) *ACS Symp. Ser.* **889** 84-97.

[9] Saha,B.C. and Bothast,R.J., (1999) *Appl. Biochem. Biotechnol.* **76** 65-77.

[10] Saha,B.C., Iten,L.B., Cotta,M.A. and Wu,Y.V., (2005) *Biotechnol. Prog.* **21** 816-822.

[11] Dien,B.S., Li,X.-., Iten,L.B., Jordan,D.B., Nichols,N.N., O'Bryan,P.J. and Cotta,M.A., (2006) *Enzyme Microb. Technol.* **39** 1137-1144.

[12] Qureshi,N., Dien,B.S., Nichols,N.N., Saha,B.C. and Cotta,M.A., (2006) *Food Bioprod. Process.* **84** 114-122.

[13] Mosier,N.S., Hendrickson,R., Brewer,M., Ho,N., Sedlak,M., Dreshel,R., Welch,G., Dien,B.S., Aden,A. and Ladisch,M.R., (2005) *Appl. Biochem. Biotechnol.* **125** 77-97.

[14] Chaudhuri,B.K. and Sahai,V., (1993) *Enzyme Microb. Technol.* **15** 513-518.

[15] Chundawat,S.P.S., Balan,V., Dale,B.E., Jones,D. and Sousa,L.D., (2007) Abstracts of Papers, *233rd ACS National Meeting,* Chicago, IL, United States, March 25-29.

[16] Jeffries,T.W., (2000) *Adv. Appl. Microbiol.* **47** 221-268.

[17] Ballesteros,M., Oliva,J.M., Negro,M.J., Manzanares,P. and Ballesteros,I., (2004) *Process Biochemistry* **39** 1843-1848.

[18] Zaldivar,J., Nielsen,J. and Olsson,L., (2001) *Appl. Microbiol. Biotechnol.* **56** 17-34.

[19] Bothast,R.J., Nichols,N.N. and Dien,B.S., (1999) *Biotechnol. Prog.* **15** 867-875.

[20] Bals,B., Dale,B. and Balan,V., (2006) *Energy Fuels* **20** 2732-2736.

[21] Xu,Z., Wang,Q., Jiang,Z., Yang,X. and Ji,Y., (2007) *Biomass Bioenergy* **31** 162-167.

[22] Xu,Y., Shen,Q., Zhong,Z. and Chen,X., (2004) *Guangpuxue Yu Guangpu Fenxi* **24** 1050-1054.

[23] Liu,R., Yu,H. and Huang,Y., (2005) *Cellulose* **12** 25-34.

[24] Laureano-Perez,L., Teymouri,F., Alizadeh,H. and Dale,B.E., (2005) *Appl. Biochem. Biotechnol.* **121-124** 1081-1099.

[25] Saravanan,S., Balasubramanian,A. and Gunsasekaran,S., (2000) *Asian Journal of Physics* **9** 480-482.

[26] Kotilainen,R.A., Toivanen,T. and Alen,R.J., (2000) *J. Wood Chem. Technol.* **20** 307-320.

[27] Kondo,T., Kataoka,Y. and Hishikawa,Y., (1998) *ACS Symp. Ser.* **688** 173-183.

[28] Zhang,J. and Pan,S., (1995) *Xianweisu Kexue Yu Jishu* **3** 22-27.

[29] Mascarenhas,M., Dighton,J. and Arbuckle,G.A., (2000) *Appl. Spectrosc.* **54** 681-686.

[30] Corredor,D.Y., Bean,S. and Wang,D., (2007) *Cereal Chem.* **84** 61-66.

[31] Corredor,D.Y., Sun,X.S., Salazar,J.M., Hohn,K.L. and Wang,D., (2008) *Journal of Biobased and Bioenergy* **2** 1-8.

[32] National Renewable Energy Laboratory (NREL). (2006). LAP 001-008. Golden, CO.

[33] American Association of Cereal Chemists., (2000) *Approved Methods of the AACC*, 10th ed, St. Paul, MN .

[34] Association of Official Analytical Chemists, (1995) *Approved Methods of the AOAC*, 15th Ed. Arlington, VA.

[35] Segal,L., Creely,J.J., Martin,A.E.J. and Conrad,C.M., (1959) *Textile Research Journal* **29** 786-794.

[36] O. Faix. (1992), in: *Methods in Lignin Chemistry* , S.Y. Lin and C.W. Dence (eds)., Springer-Verlag, Berlin, pp. 83-93.

[37] Pandey,K.K., (1999) *J Appl Polym Sci* **71** 1969-1975.

[38] Sene,C.F.B., McCann,M.C., Wilson,R.H. and Grinter,R., (1994) *Plant Physiol.* **106** 1623-1631.

[39] Sun,R. and Tomkinson,J., (2004) *Sep. Sci. Technol.* **39** 391-411.

[40] Sjöström,E., (1981). *Wood chemistry : fundamentals and appl*ications, Academic Press, New York .

[41] Stewart,D., Wilson,H.M., Hendra,P.J. and Morrison,I.M. (1995) *J. Agric. Food Chem.* **43** 2219-2225.

[42] R.H. Atalla, U.P. Agarwal and J.S. Bond. (1992) in *Methods in Lignin Chemistry.* S.Y. Lin and C.W. Dence (eds), Springer-Verlag, Berlin, pp. 162-176.

[43] Michell,A.J., (1990) *Carbohydr. Res.* **197** 53-60.

[44] Reddy,N. and Yang,Y. (2007) *J. Agric. Food. Chem.* **55** 5569-5574.

[45] Kim,T.H., Lee,Y.Y., Sunwoo,C. and Kim,J.S. (2006) *Appl. Biochem. Biotechnol.* **133** 41-57.

[46] Evert,R.F. (2006) *Esau's Plant Anatomy*, 3rd ed., John Wiley and sons, New Jersey .

[47] Franz, G., and Blaschek, W. (1990), in: *Methods in Plant Biochemistry.* P.M. Dey (ed). Academic Press Limited, San Diego, CA, pp. 291-322.

[48] Kasai,N. and Kakudo,M. (2005) *X-Ray Diffraction by Macromolecules*, Springer, Japan.

[49] Ardizzone,S., Dioguardi,F.S., Mussini,T., Mussini,P.R., Rondinini,S., Vercelli,B. and Vertova,A. (1999) *Cellulose* **6** 57-69.

[50] Soltys,J., Lisowski,L. and Knapczyc,J. (1984) *Acta Pharmaceutica Technologica,* **30** 174-180.

[51] Monties, B. (1989). in: *Methods in Plant Biochemistry*. J.B. Harborne (ed.), Academic Press, San Diego, CA, pp. 113-157.